coatings

MDPI

Article

The Electronic Structure and Optical Properties of $CdGeAs_2$ Crystal: A DFT and HSE06 Study

Suqin Xue [1,†], Jing Ning [2,†], Bohang Zhang [2], Qiao Wu [1], Fuchun Zhang [2,*] and Weibin Zhang [3,*]

1 Network Information Center, Yan'an University, Yan'an 716000, China
2 School of Physics and Electronic Information, Yan'an University, Yan'an 716000, China
3 College of Physics and Electronics Information, Yunnan Key Laboratory of Opto-Electronic Information Technology, Yunnan Normal University, Kunming 650500, China
* Correspondence: yadxzfc@yau.edu.cn (F.Z.); 220001@ynnu.edu.cn (W.Z.); Tel.: +86-1832-991-8036 (F.Z.); +86-1898-726-7036 (W.Z.)
† These authors contributed equally to this work.

Abstract: The electronic structural and optical properties of $CdGeAs_2$ crystals are calculated by using the Perdew–Burke–Ernzerhof (PBE) functional within generalized gradient approximation (GGA) and the Heyd–Scuseria–Ernzerhof (HSE06) functional. The results show that $CdGeAs_2$ is an optical crystal with a direct bandgap of 0.71 eV by using the HSE06 functional method, which is closer to the experimental value. The Mulliken population and differential charge density analysis indicate that the Ge–As and Cd–As bonds have covalent properties, and that the covalent bond of Cd–As is visibly stronger than that of the Ge–As bond. The optical properties show that the $CdGeAs_2$ crystal has strong absorption and reflection in the ultraviolet region and strong transmittance in the infrared region. The average static refractive index of $CdGeAs_2$ is 2.96, and the static birefractive index is 0.08. The results show that $CdGeAs_2$ is an excellent optical material of potential applications in the middle and far infrared.

Keywords: $CdGeAs_2$; density functional theory; electronic structure; optical properties

Citation: Xue, S.; Ning, J.; Zhang, B.; Wu, Q.; Zhang, F.; Zhang, W. The Electronic Structure and Optical Properties of $CdGeAs_2$ Crystal: A DFT and HSE06 Study. *Coatings* **2022**, *12*, 1778. https://doi.org/10.3390/coatings12111778

Academic Editors: Claudia Barile and Gilda Renna

Received: 28 October 2022
Accepted: 16 November 2022
Published: 21 November 2022

1. Introduction

The $CdGeAs_2$ crystal is a typical II-IV-V_2 ternary chalcopyrite semiconductor compound, which has a wide transparent range (2.3~18 μm) [1], the highest nonlinear optical coefficient (d_{36} = 236 pm/V) [2], a large birefringence ($n_e - n_o \approx 0.09$) [3], and high thermal conductivity (0.04 W/(cm·K)) [4]. Therefore, the $CdGeAs_2$ crystal can be widely used in the production of frequency-doubling and frequency-mixing infrared parametric oscillators [5]. It has broad application prospects in the military and civil fields such as optical devices [6], laser technology [7–9], infrared medical instruments [10], and so on. It is a middle and far infrared nonlinear optical crystal with great development prospects, which has attracted much attention at home and abroad.

Since the late 1960s, there have been many experimental studies on $CdGeAs_2$ crystals, including photoluminescence [11], optical parametric oscillator [12], p-type $CdGeAs_2$ luminescence and optical absorption [13], $CdGeAs_2$ defects and doping [14,15], etc. However, compared to the experimental research, there are few theoretical studies. Most researchers focus on the electronic structure of the $CdGeAs_2$ crystal, and the studies on the optical properties are relatively simple and incomplete. For example, Yu et al. [16] calculated the band structure, density of states, charge density, the dielectric function, and other properties of the $CdGeAs_2$ crystal by using a pseudopotential plane wave method. The bandgap value calculated by the local density approximation (LDA) method was 0.16 eV, and the GW approximation (GWA, where G is the Green' s function and W is the screened coulomb interaction) method was 0.35 eV. In addition, only the dielectric function is calculated in the linear optical response. Ma et al. [17] calculated the electronic structure, optical properties, and elastic properties of the $CdGeAs_2$ crystal using the GGA–PBE and LDA methods, in which the calculated bandgap values were 0.23 eV (GGA–PBE) and 0.41 eV (LDA), and only the dielectric function and refractive index were studied in the study of optical properties. Yu et al. [18] studied the structure, electronic, and optical properties of the $CdGeAs_2$ crystal by the HSE06 method, and the calculated bandgap value was 0.548 eV, which indeed effectively reduced the theoretical error of the bandgap. However, the optical properties of the $CdGeAs_2$ crystal were rarely studied and analyzed. According to a significant portion of the literature, it is found that the bandgap of the crystal can be seriously underestimated by the theoretical calculation based on the GGA–PBE and LDA methods. Which is quite different from the bandgap value obtained by the experimental research (0.67 eV [19]). However, we can use some accurate hybrid functionals of exchange potentials to obtain accurate values of bandgap. The experimental studies show that optical properties are very important factors affecting the practical application of the $CdGeAs_2$ crystal, so it is very necessary to conduct a comprehensive theoretical study on the optical properties of the $CdGeAs_2$ crystal, which can provide an important theoretical reference for the improvement of crystal optical quality, experimental preparation, and application.

In this work, the electronic and optical properties of the $CdGeAs_2$ crystal are calculated by the GGA–PBE [20] and HSE06 [21] methods, respectively. According to the calculated results, we can obtain more accurate electronic structures and compare them with experimental values. On the basis of calculating the dielectric function of $CdGeAs_2$, the reflectance spectrum, the absorption spectrum, the complex refractive index, the birefringence, and the energy loss function of $CdGeAs_2$ was calculated, and the relationship between electronic structure and optical properties were systematically studied. It has important guiding significance for the improvement of the experimental preparation and practical application of $CdGeAs_2$.

2. Theoretical Model and Calculation Method

2.1. Theoretical Model

The $CdGeAs_2$ crystal belongs to the II-IV-V_2 chalcopyrite structure semiconductor, and its crystal structure can be regarded as the superposition of two binary cubic sphalerite crystal cells, which is equivalent to expanding the c-axis direction of sphalerite by two times. In fact, there is only one cation in the sphalerite structure, while there are two different types of cations in the ternary chalcopyrite structure, which causes the decrease in the symmetry of the chalcopyrite structure system. In general, the II-V atomic bond lengths ($d_{II\text{-}V}$) and the IV-V atomic bond lengths ($d_{IV\text{-}V}$) are not equal, resulting in two different structural deformations: The first deformation is a change in the occupation of anions, with the anion having an inner coordinate u = 0.25 for sphalerite and $u = 0.25 + (d^2{}_{II\text{-}V} - d^2{}_{IV\text{-}V})/a^2$ for chalcopyrite, where a is the lattice constant along the x or y directions [22]. The second deformation is that the lattice constant (c) along the z direction is not equal to 2a, which means that c/a is not equal to 2. For the II-IV-V_2 chalcopyrite structure, u = 0.214~0.304, c/a = 1.769~2.016 in most cases, and the structure parameters of the $CdGeAs_2$ crystal are also within this boundary range. In the crystal structure of $CdGeAs_2$, the Cd, Ge, and As atoms form a tetrahedron, the anion As^{3-} is located in the center of the tetrahedron, and the cations Cd and Ge occupy the four top angles of the tetrahedron. In each layer, the cations Cd and Ge are arranged in a certain order [23]. The structural model of $CdGeAs_2$ is shown in Figure 1.

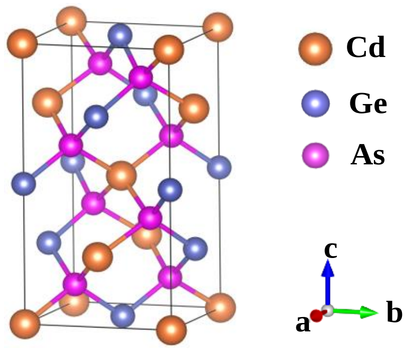

Figure 1. The structural model of $CdGeAs_2$ (orange sphere is Cd atom, blue sphere is Ge atom, pink sphere is As atom).

2.2. Calculation Method

In this work, we calculated the structural optimization and performance of the crystal using the Vienna ab-initio Simulation Package (VASP) [24]. The GGA–PBE method is used to accurately calculate the total energy and exchange-related interactions. We use the HSE06 method to avoid the underestimation of bandgap values and the overestimation of optical responses in standard density functional theory (DFT) [25] calculations. The valence electrons of Cd, Ge, and As are $4d^{10}5s^2$, $4s^24p^2$, and $4s^24p^2$, respectively. In the electron self-consistent iterative cycle, the criterion for convergence is 1×10^{-5} eV/Å for the total energy and 1×10^{-6} eV for the atomic relaxation. The truncation energy is set to 520 eV. The k-points grid is set to $6 \times 6 \times 4$ according to the Monkhorst–Pack scheme, which can ensure that the system always converges well.

3. Results and Discussion

3.1. Geometric Optimization Results

In order to obtain reasonable calculation results, a stable crystal structure is necessary. The lattice parameters of the stable structure are obtained according to the principle of minimizing the total cell energy, and the obtained crystal cell parameters are shown in Table 1. The lattice constants of the stable structure of the $CdGeAs_2$ crystal are as follows: $a = b = 6.041$ Å, $c/a = 1.887$, $u = 0.278$. The optimized lattice constant a is close to the experimental value of 5.94 [26], the relative error of both a and c values is ~1.70%, and the relative error of the u value is 0.4%. Due to the fact that the optimized crystal is an ideal crystal, the zero-point motion and thermal effect are not considered, so there is a certain error with the experimental value.

Table 1. The structural optimization results of $CdGeAs_2$.

Parameter	This Work	Experimental Value [26]	Relative Error
$a = b$/Å	6.041	5.94	1.7%
c/Å	11.407	11.22	1.7%
u	0.278	0.279	0.4%
$\alpha = \beta = \gamma$ (°)	90	-	-

3.2. Electronic Structure

The band structure of $CdGeAs_2$, calculated by the GGA–PBE and HSE06 methods, are shown in Figure 2, and the Fermi level (E_f) is set to zero. These particular points on the x-axis represent points of high symmetry in the Brillouin zone (BZ). For the quadrilateral structure of $CdGeAs_2$, Z = (0.3, 0.3, 0.3), Γ = (0, 0, 0), X = (0.3, 0, 0), P = (0.3, −0.3, 0.3), and N = (0.3, −0.3, 0). The characteristic energy values of the top of the valence band (E_V) and the bottom of the conduction band (E_C) in the BZ of $CdGeAs_2$ are shown in Table 2. It can be seen from the values in the table that the top of the valence band (VBM) and the bottom of the conduction band (CBM) are both at the Γ point. Therefore, $CdGeAs_2$ is a direct bandgap semiconductor material. The bandgap values (E_g) of $CdGeAs_2$ calculated using the GGA–PBE and HSE06 methods are shown in Table 3 and compared with the experimental value. The E_g calculated by the GGA–PBE method is 0.079 eV, and the E_g calculated using the HSE06 method is 0.710 eV. Compared with the experimental values (0.67 eV [18] and 0.53 eV [27]), the average relative error calculated by the GGA–PBE method is 86.65%, which seriously underestimates the bandgap value, while the average relative error calculated by the HSE06 method is 19.97%, which is closer to the experimental value. The relevant values are listed in Table 3. When the E_g is calculated by the GGA method, the self-interaction of electrons does not cancel completely in the exchange-correlation potential, and its eigenfunction is discontinuous, so the GGA method will underestimate E_g. When the calculation does not include the spin–orbit interactions, the three lower conduction band (CB) states at the Γ point are Γ_1, Γ_3, and Γ_2. The energy splitting value between Γ_2 and Γ_3 is 0.49 eV, which is very close to the 0.46 eV calculated by Limpijumnong et al. [28]. At point Γ, the top of the valence band (VB) consists of two symmetric levels Γ_4 and Γ_5, the latter being a double degenerate level. Due to the crystal field (*CF*), the non-degenerate Γ_4 and double-degenerate Γ_5 in the chalcopyrite structure originate from the Γ_{15} level of the zinc–blende structure [29]. Therefore, the crystal field splitting can be expressed as $\Delta CF = \varepsilon(\Gamma_5) - \varepsilon(\Gamma_4)$. The calculated ΔCF value of $CdGeAs_2$ is 0.227 eV, which is very close to the experimental value (0.21 eV) [30].

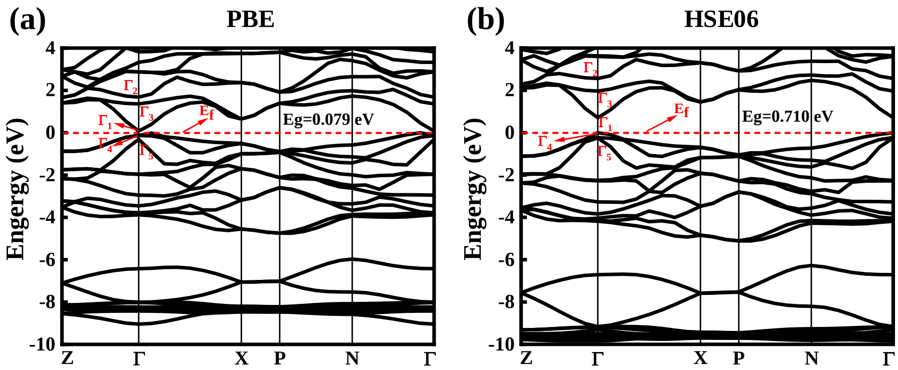

Figure 2. The band structures of $CdGeAs_2$. (**a**) GGA–PBE, (**b**) HSE06.

Table 2. The characteristic energy values of E_V and E_C in the BZ of $CdGeAs_2$.

Method	Parameter	Z	Γ	X	P	N
GGA–PBE	E_V (eV)	1.400	0.079	0.650	1.390	1.730
	E_C (eV)	−0.875	0	−0.509	−0.891	−0.580
HSE06	E_V (eV)	2.120	0.710	1.450	2.040	2.480
	E_C (eV)	−1.110	0	−0.686	−1.050	−0.730

Table 3. The E_g of $CdGeAs_2$ calculated by GGA–PBE and HSE06 methods.

Method	This Work (eV)	Experimental Value (eV) [18,27]	Mean Relative Error
PBE	0.079	0.67 or 0.53	86.65 %
HSE06	0.710	0.67 or 0.53	19.97%

We analyze the distribution of electrons per atomic orbital by calculating the total density of states (TDOSs) and partial density of states (PDOSs). Figure 3 shows the TDOSs and PDOSs of $CdGeAs_2$ calculated using the GGA–PBE method and the HSE06 method. As can be seen from the figure, the VB of $CdGeAs_2$ can be divided into three regions: In the lower VB (−13~−11 eV), it is mainly composed of As-4*s* states, with a small amount of Ge-4*p* and Ge-4*s* orbital hybridization. In the intermediate VB (−10~−6 eV), it is mainly composed of Ge-*4s* and Cd-*4d* electronic states. The higher VB (−5~0 eV) is mainly derived from the As-*4p* and Ge-*4p* states. The CB is mainly composed of the As-*4s*, As-*4p*, Ge-*4p*, and Ge-*4s* orbitals. The density of states (DOSs) near the VBM and the CBM are mainly derived from As atoms, as shown in Figure 3. In the experiment, the change of As content will change the bandgap of the single crystal, and then affect the optical transmittance. Therefore, the content of As can be increased appropriately when preparing a $CdGeAs_2$ single crystal.

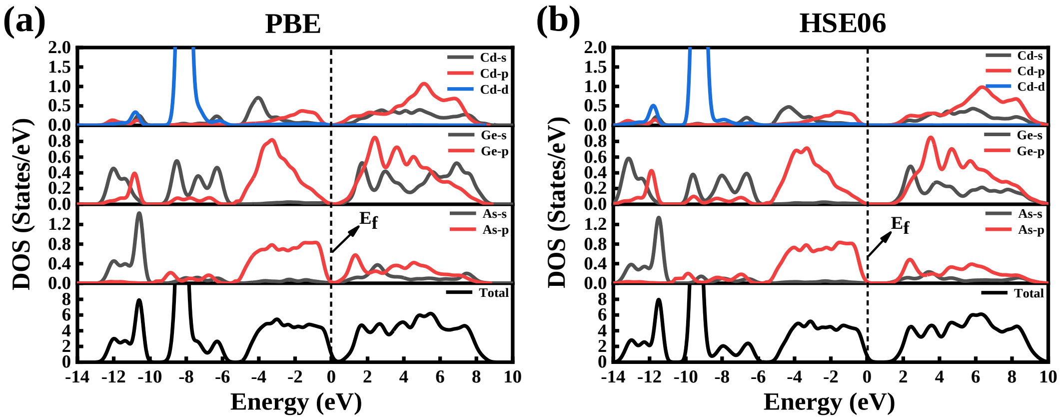

Figure 3. The total and partial density of states of $CdGeAs_2$. (**a**) GGA–PBE, (**b**) HSE06.

3.3. Mulliken Charge Population Analysis

We computed the Mulliken population analysis, which allows us to understand the interaction and bonding between atoms. The Mulliken charge, bond lengths, and bond lattice numbers of $CdGeAs_2$ crystals calculated using the GGA–PBE and HSE06 methods are shown in Table 4. From the calculation results, it can be seen that the charge transfer of the $CdGeAs_2$ compounds is from the Cd and Ge atoms into the As atoms. Taking the calculation results of the HSE06 method as an example: the Cd and Ge atoms carry positive charges of 0.19 and 0.13, respectively. The Cd and Ge atoms are very capable of losing electrons, while the As atoms carry negative charges of 0.16 and are very capable of gaining electrons. The bond characteristics (ionic bonds or covalent) can be assessed and determined using overlapping populations. In general, a zero number of the chemical bond population indicates an ideal ionic bond, while a positive value is proportional to the covalency of the bond. In Table 4, the populations of As atoms with Cd atoms and Ge atoms are 0.67 and 0.26, respectively, which confirmed that the covalency of the Cd–As bond and that the Ge–As bond of $CdGeAs_2$ compounds is weak, as well as that the covalency of the Cd–As bond is higher than that of the Ge–As bond.

Table 4. The population analysis of $CdGeAs_2$.

Methods	Atom	s	p	d	Total	Charge	Bond	Length (Å)	Population
PBE	Cd	0.95	1.08	9.97	12.00	−0.00	Cd–As	2.47100	0.27
	Ge	1.17	2.36	0	3.53	0.47	Ge–As	2.67279	0.04
	As	1.67	3.56	0	5.23	−0.23	-	-	-
HSE06	Cd	0.78	1.06	9.97	11.81	0.19	Cd–As	2.46677	0.67
	Ge	1.53	2.34	0	3.87	0.13	Ge–As	2.68291	0.26
	As	1.43	3.73	0	5.16	−0.16	-	-	-

3.4. The Differential Charge Density

Figure 4 shows the differential charge density of $CdGeAs_2$ to visualize the bond properties. Figure 4a shows the 3D differential charge density of $CdGeAs_2$, where green represents electron loss and yellow represents electron gain. It can be seen that electrons accumulate near the As atom, and that the Cd atom is surrounded by green, indicating that it has a strong ability to lose electrons. The Cd–As atoms form strong chemical bonds with each other, while the Ge–As atoms form weak bonds with each other. Figure 4b shows the 2D plan differential charge density of $CdGeAs_2$. Figure 3 shows that the intermediate region (-10~-6 eV) is mainly derived from the Cd-*4d* states and is thus strongly localized around the Cd atom. As can be seen from Figure 4b, there is an obvious electron density overlap between the As atom, the Ge atom, and the Cd atom, which indicates that the bonds Ge–As and Cd–As have covalent properties. The density lines in the 2D differential charge map indicate that the Cd–As bond has stronger covalent properties than the Ge–As bond. This result is consistent with the Mulliken population analysis.

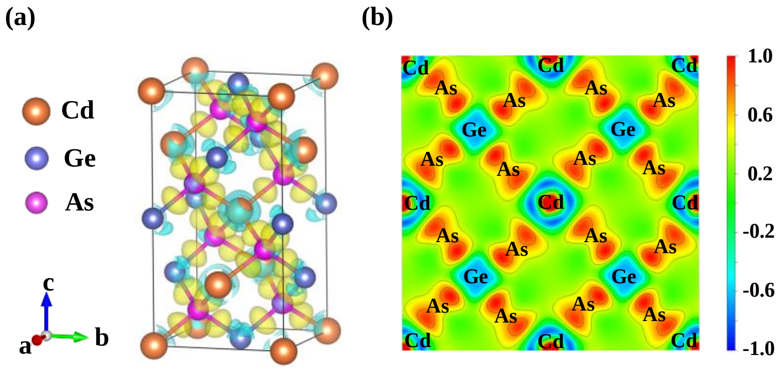

Figure 4. The differential charge density of $CdGeAs_2$. (**a**) 3D, (**b**) 2D.

3.5. Optical Properties

Generally, the complex dielectric function can be used to express the macroscopic optical properties of solids [31]:

$$\varepsilon(\omega) = \varepsilon_1(\omega) + i\varepsilon_2(\omega) \tag{1}$$

where $\varepsilon_1(\omega)$ is the real part, and $\varepsilon_2(\omega)$ is the imaginary part. The imaginary part $\varepsilon_2(\omega)$ can be calculated according to the following formula:

$$\varepsilon_2(\omega) = \frac{4\pi^2}{m^2\omega^2}\sum_{V,C}\left\{\int_{BZ} d^3k\frac{1}{\pi}|e\cdot M_{CV}(k)|^2 \times \delta[E_C(k) - E_V(k) - \hbar\omega]\right\} \tag{2}$$

where C and V represent CB and VB, corresponding to the intrinsic energy $E_C(k)$ and $E_V(k)$ of the CB and VB, respectively. M_{CV} stands for transition matrix element, ω is the electromagnetic wave frequency, and k is the electron wave vector. Real $\varepsilon_1(\omega)$ is derived from imaginary $\varepsilon_2(\omega)$ using the Kramers–Krönig relation:

$$\varepsilon_1(\omega) = 1 + \frac{2}{\pi}P\int_0^\infty \frac{\omega'\varepsilon_2(\omega')}{\omega'^2 - \omega^2}d\omega' \tag{3}$$

where P is the principal value of the integral. The imaginary and real parts of the dielectric function can be used to calculate other optical properties, such as refractive index $n(\omega)$, reflectivity $R(\omega)$, conductivity function $\sigma(\omega)$, and energy loss spectrum $L(\omega)$. The formula is as follows:

$$n(\omega) = \left[\frac{\varepsilon_1(\omega)}{2} + \frac{\sqrt{\varepsilon_1^2(\omega) + \varepsilon_2^2(\omega)}}{2}\right]^{1/2} \tag{4}$$

$$R(\omega) = \left|\frac{\sqrt{\varepsilon(\omega)} - 1}{\sqrt{\varepsilon(\omega)} + 1}\right|^2 \tag{5}$$

$$\sigma(\omega) = \frac{\omega}{4\pi}\varepsilon_2(\omega) + i\left(\frac{\omega}{4\pi} - \frac{\omega}{4\pi}\varepsilon_1(\omega)\right) \tag{6}$$

$$L(\omega) = \frac{\varepsilon_2(\omega)}{\varepsilon_1^2(\omega) + \varepsilon_2^2(\omega)} \tag{7}$$

In this paper, the GGA–PBE and HSE06 methods are used to calculate the dielectric function of $CdGeAs_2$ material. Due to the symmetry of the crystal, the dielectric function is decomposed into two components. E⊥c is the electric field along the x and y directions (the electric field perpendicular to the optical axis), and E//c corresponds to the z direction (the electric field parallel to the optical axis). Figure 5a,c show the real part $\varepsilon_1(\omega)$ of the dielectric function calculated by the GGA–PBE and HSE06 methods, respectively. When $\varepsilon_1(\omega)$ photon energy tends to 0, the average static permittivity ($\varepsilon_1{}^{ave}$ (0)) of $CdGeAs_2$ calculated using the GGA–PBE and HSE06 methods are 18.42 and 16.57, respectively. The experimental value of the dielectric function is 15.4 [32], and the relative errors are 19.61% (GGA–PBE) and 7.59% (HSE06). Therefore, the results calculated by the HSE06 method are closer to the experimental value.

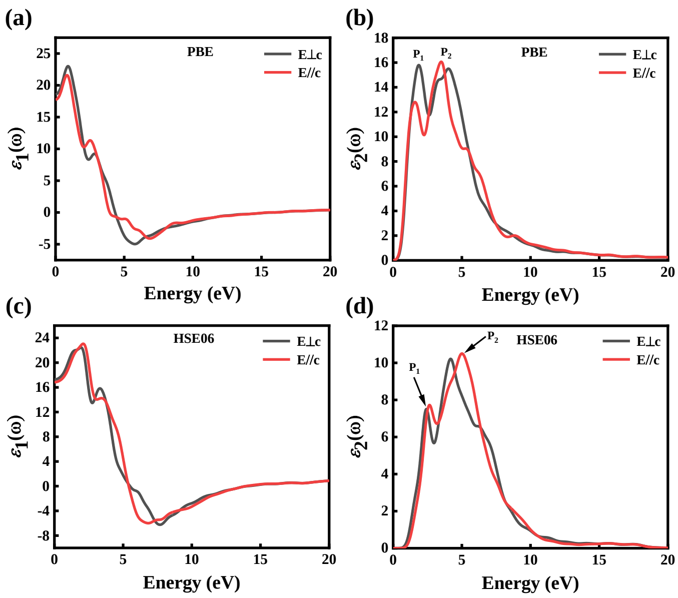

Figure 5. (**a**) The real part and (**b**) the imaginary part of the dielectric function of $CdGeAs_2$ of GGA–PBE; (**c**) the real part and (**d**) the imaginary part of the dielectric function of $CdGeAs_2$ of HSE06.

Figure 5b,d show the imaginary part $\varepsilon_2(\omega)$ of the dielectric function calculated by the GGA–PBE and HSE06 methods, respectively. $\varepsilon_2(\omega)$ determines the linear response of the light field. The basic absorption edges, calculated by the GGA–PBE and HSE06 methods, are 0.09 eV and 0.72 eV, respectively, which is connected with the electron transition from the VBM to the CBM. The dielectric spectrum can be divided into four regions: 0~0.6 eV and >17 eV are the transparent areas, 0.6~10 eV is the absorption area, 10~17 eV is the reflex area. In the region above the absorption edge, there are two main dielectric peaks, namely P_1 and P_2 in $\varepsilon_2(\omega)$. The photon energies corresponding to the dielectric peaks calculated by GGA–PBE are 1.94 eV and 4.81 eV, respectively, while those calculated by HSE06 are 2.65 eV and 5.61 eV, respectively. As can be seen from Figure 3, peak P_1 is mainly derived from the electronic transition of the As-*4p* states between the CB and VB, while peak P_2 is generated by the electronic transition of the As-*4p* and Ge-*4p* orbitals between the CB and VB.

In this paper, the GGA–PBE and HSE06 methods are used to calculate the reflection and absorption spectra of $CdGeAs_2$ crystals, as shown in Figure 6. The $CdGeAs_2$ reflectance spectrum obtained according to Equation (5) is shown in Figure 6a,b. The reflectance shows obvious anisotropy along different directions. Due to the band transition of $CdGeAs_2$, the reflectance is proportional to the energy change. The reflectance reaches its maximum value around 10.0 eV. With increasing energy, the reflectance rapidly decreases to 0. In conclusion, the $CdGeAs_2$ crystal has low reflectance in the infrared band.

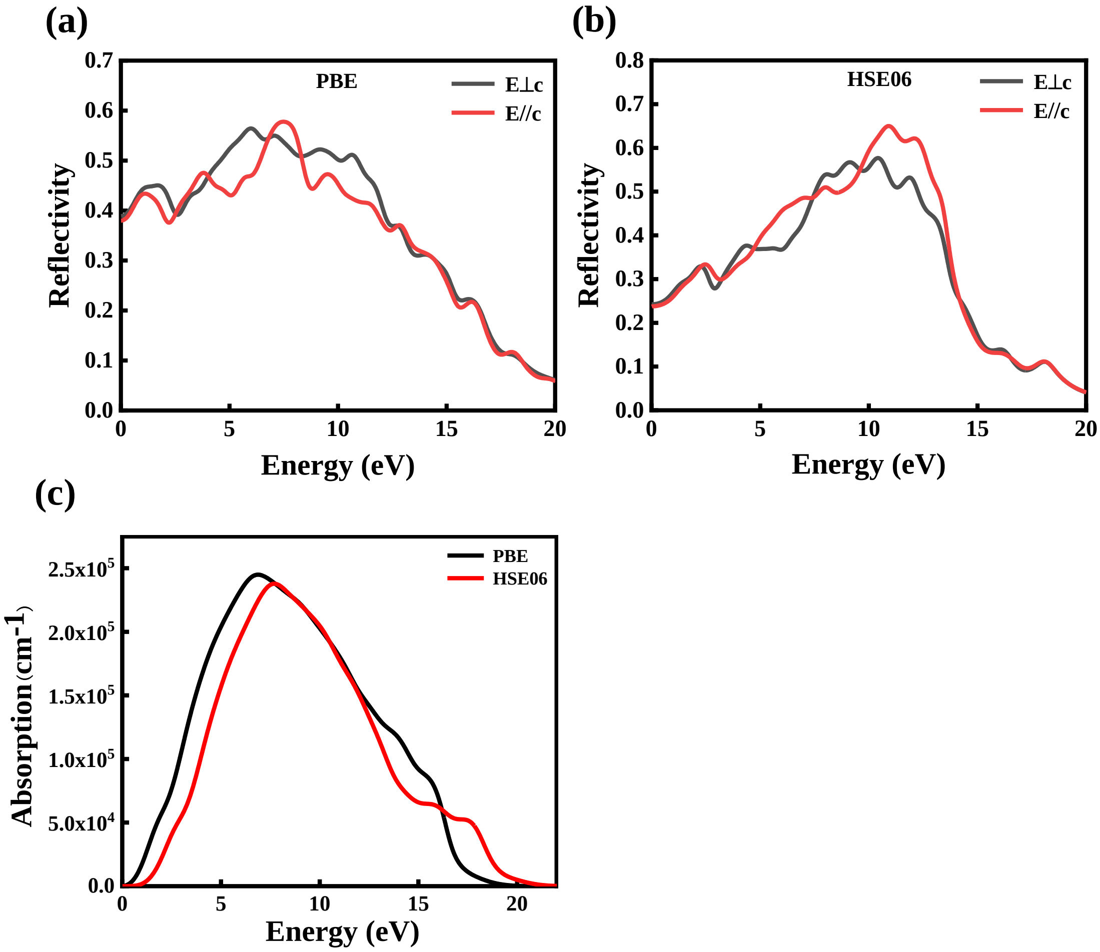

Figure 6. (**a**,**b**) The reflectance spectrum and (**c**) the absorption spectrum of $CdGeAs_2$.

The absorption spectrum of $CdGeAs_2$ obtained according to Equation (6) is shown in Figure 6c. The absorption calculated by the PBE and HSE06 methods starts at about 0.09 eV and 0.72 eV, respectively, which corresponds to the bandgap value of the material. The strongest absorption peak calculated by the GGA–PBE method appears at 6.82 eV, and the strongest absorption peak calculated by the HSE06 method appears at 7.75 eV.

The refractive index and the extinction coefficient of $CdGeAs_2$, calculated by the GGA–PBE and HSE06 methods, are shown in Figure 7. The propagation speed of light wave in $CdGeAs_2$ determines the refractive index (n), and the attenuation of light wave determines the extinction coefficient (k). The average static refractive index calculated by the GGA–PBE method and the HSE06 method are 4.67 and 2.96, respectively. The extinction coefficients calculated by the GGA–PBE method have peaks at 2.07 eV and 4.95 eV. The peak values calculated by the HSE06 method were 2.79 eV and 5.93 eV, which is consistent with $\varepsilon_2(\omega)$.

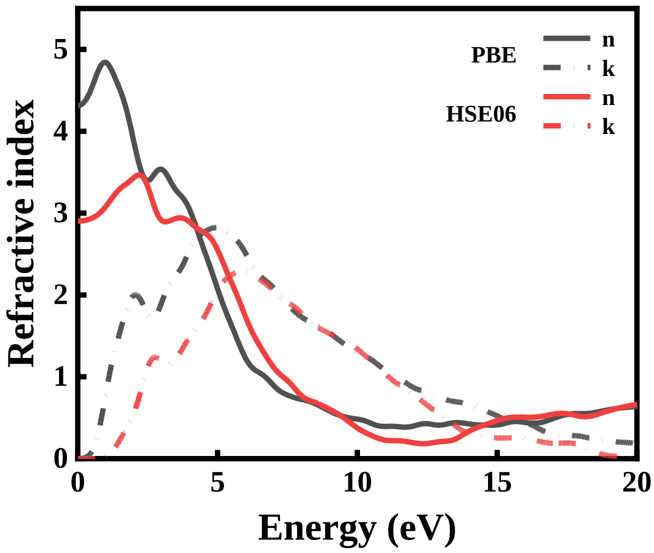

Figure 7. The complex refractive index of $CdGeAs_2$.

The birefringence (Δn) of the $CdGeAs_2$ crystal calculated using the GGA–PBE and HSE06 methods is shown in Figure 8. The birefringence is expressed as the difference between two or three main refractive indices ($\Delta n = n_i - n_j$) in heterogeneous bodies. The birefringence is an important physical quantity in measuring nonlinear crystal properties. The most suitable birefringence range of mid-infrared nonlinear optical crystal is $0.04 < \Delta n < 0.1$ [33]. According to Figure 8a, the static birefringence of $CdGeAs_2$ calculated using the GGA–PBE method is 0.11, which reaches the maximum value of 0.54 at 4.09 eV. As can be seen from Figure 8b, the static birefringence of $CdGeAs_2$ calculated using the HSE06 method is 0.08, which reaches the maximum value of 0.33 at 7.59 eV. At the wavelength of 10 μm, the experimental value of birefringence is 0.0864 [34]. The relative errors are 27.31% (GGA–PBE) and 7.41% (HSE06), so the result calculated by the HSE06 method is closer to the experimental value. By comparing the results calculated using the GGA–PBE and HSE06 methods, it is found that the bandgap of the $CdGeAs_2$ crystal is underestimated by the GGA–PBE method, which leads to the increase in the average static refractive index and birefringence in the mid-far infrared region.

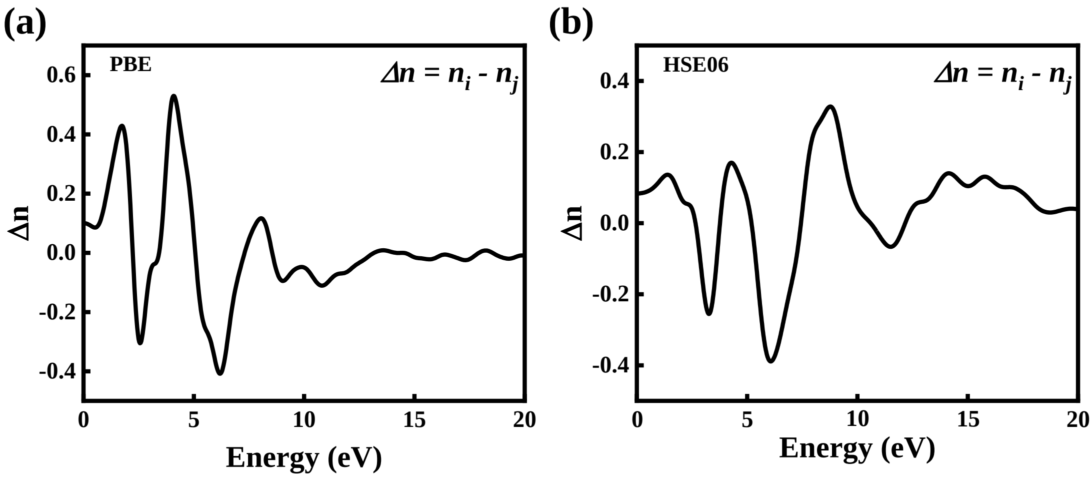

Figure 8. The birefringence of $CdGeAs_2$. (**a**) GGA–PBE, (**b**) HSE06.

According to Equation (7), the energy loss function of $CdGeAs_2$ is calculated, which describes the energy loss of the electrons when they pass through the medium. The energy loss spectrum of $CdGeAs_2$ is shown in Figure 9. The maximum energy loss peak at 16.36 eV is calculated by the GGA–PBE method, and its value is 8.09. The result obtained by the HSE06 shows that the maximum energy loss occurs at 14.06 eV, and its value is 4.08. In addition, it can be concluded from the band structure and the DOS analysis that the highest peak comes from the transition of the As-*4s*, Ge-*4s*, and Ge-*4p* orbitals from the VB to the CB.

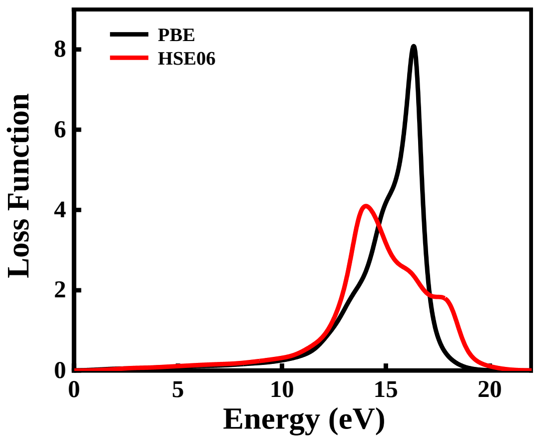

Figure 9. The energy loss function of $CdGeAs_2$.

4. Conclusions

In this work, the electronic structure and optical properties of the $CdGeAs_2$ crystal are calculated using GGA–PBE and HSE06 methods. The results show that the relative error of the bandgap value calculated by GGA–PBE method is large, while the result calculated by the HSE06 method is closer to the experimental value. The calculation results of the DOSs show that the VBM is mainly composed of As-*4p* and Ge-*4p* states, and that the CBM is mainly composed of the orbitals of As-*4s*, As-*4p*, Ge-*4s*, and Ge-*4p*. The Mulliken population analysis and differential charge density results show that the bonds Ge–As and Cd–As are covalent. Moreover, the covalency of the Cd–As bond is higher than that of the Ge–As bond. In addition, we systematically calculate the optical properties of $CdGeAs_2$. The relative errors of average static permittivity calculated using GGA–PBE and HSE06 are 19.61% and 7.59%, respectively, and the relative errors of static birefringence are 27.31% and 7.41%, respectively. The results of the optical properties show that the $CdGeAs_2$ crystal has strong absorption and reflection in the ultraviolet region, along with strong transmission and excellent birefringence in the infrared region. In summary, the HSE06 method is more suitable for calculating the electronic structure and optical properties of the $CdGeAs_2$ crystal. Meanwhile, the theoretical calculation results prove that the $CdGeAs_2$ crystal is an excellent medium and far infrared optical crystal material, and the calculation results provide an important theoretical reference for the improvement of crystal optical quality, experimental preparation, and its application.

Author Contributions: F.Z. and W.Z. supervised the research. J.N. and S.X. calculated a series of properties of the material and wrote the first draft. B.Z. and Q.W. analyzed the data and revised the paper. All authors have read and agreed to the published version of the manuscript.

Funding: This research was funded by the National Natural Science Foundation of China (Grant No. 62264015, 52262042), the National Science Foundation of Shaanxi Province, China (2021JQ-635), the Scientific Research Program of Yan'an University (YDQ2020-08), and the Scientific and Technological Innovation Team (2017CXTD-01).

Institutional Review Board Statement: This work does not involve humans or animals.

Informed Consent Statement: Not applicable.

Data Availability Statement: All data are presented in the form of charts in the article.

Conflicts of Interest: The authors declare no conflict of interest.

References

1. Huang, W.; Zhao, B.; Zhu, S.; He, Z.; Chen, B.; Yu, Y. Vibrational modes of chalcopyrite $CdGeAs_2$ crystal. *Mater. Res. Bull.* **2016**, *81*, 107–113. [CrossRef]
2. Huang, W.; Zhao, B.; Zhu, S.; He, Z.; Chen, B.; Zhen, Z.; Pu, Y. Correlation between dislocation etch pits, carrier concentration and optical absorption in $CdGeAs_2$ grown by modified Vertical Bridgman method. *J. Alloys Compd.* **2016**, *656*, 818–824. [CrossRef]
3. Pu, Y.; Zhu, S.; Zhao, B.; He, Z.; Chen, B.; Huang, W. Growth and characterization of Cr-doped $CdGeAs_2$ crystal. *J. Cryst. Growth* **2017**, *467*, 150–154. [CrossRef]
4. Li, J.; Zhu, S.; Zhao, B.; He, Z.; Chen, B. XPS Analysis and Determination of Surface Damage Layer of $CdGeAs_2$ Single Crystal. *Rare Met. Mater. Eng.* **2015**, *44*, 844–847.
5. Vodopyanova, K.L.; Knippels, G.M.H.; van der Meer, A.F.G.; Maffetonec, J.P.; Zwieback, I. Optical parametric generation in CGA crystal. *Opt. Commun.* **2002**, *202*, 205–208. [CrossRef]
6. Yu, Y.; Zhao, B.; Zhu, S.; Gao, T.; Hou, H. Ab initio vibrational and dielectric properties of chalcopyrite $CdGeAs_2$. *Solid State Sci.* **2011**, *13*, 422–426. [CrossRef]
7. Mei, D.; Jiang, J.; Liang, F.; Zhang, S.; Wu, Y.; Sun, C.; Xue, D.; Lin, Z. Design and Synthesis of Nonlinear Optical Material with Wide Band Gap: From SrB_4O_7 to $BaAl_4S_7$. *J. Mater. Chem. C* **2018**, *6*, 2684–2689. [CrossRef]
8. Lin, Z.; Jiang, X.; Kang, L.; Gong, P.; Luo, S.; Lee, M. First-principles materials applications and design of nonlinear optical crystals. *J. Phys. D* **2014**, *47*, 253001. [CrossRef]
9. Bera, T.K.; Song, J.H.; Freeman, A.J.; Jang, J.I.; Ketterson, J.B.; Kanatzidis, M.G. Soluble Direct-Band-Gap Semiconductors $LiAsS_2$ and $NaAsS_2$: Large Electronic Structure Effects from Weak As···S Interactions and Strong Nonlinear Optical Response. *Angew. Chem. Int. Ed.* **2008**, *47*, 7828–7832. [CrossRef]
10. Lei, Y.; Yu, M.; Li, J.; Wu, J.; Chen, B.; Yu, Y.; Huang, W.; He, Z. Synthesis, growth and mechanical properties of mid-infrared nonlinear optical crystal $CdGeAs_2$. *J. Cryst. Growth* **2021**, *562*, 126060. [CrossRef]
11. Bai, L.; Xu, C.; Nagashio, K.; Yang, C.; Feigelson, R.S.; Schunemann, P.G.; Giles, N.C. Photoluminescence of n-type $CdGeAs_2$. *J. Phys. Condens. Matter.* **2005**, *17*, 5687–5696. [CrossRef] [PubMed]
12. Huang, W.; Zhao, B.; Zhu, S.; He, Z.; Chen, B.; Li, J.; Yu, Y.; Tang, J.; Liu, W. Effect of thermal annealing on the optical properties of $CdGeAs_2$ wafers. *J. Cryst. Growth* **2013**, *362*, 291–295. [CrossRef]
13. Bai, L.; Poston, J.A.; Schunemann, P.G.; Nagashio, K.; Feigelson, R.S.; Giles, N.C. Luminescence and optical absorption study of p-type $CdGeAs_2$. *J. Phys. Condens. Matter.* **2004**, *16*, 1279–1286. [CrossRef]
14. Blanco, M.A.; Costales, A.; Luaña, V.; Pandey, R. Theoretical study of the group-IV antisite acceptor defects in $CdGeAs_2$. *Appl. Phys. Lett.* **2004**, *85*, 4376–4378. [CrossRef]
15. Garces, N.Y.; Giles, N.C.; Halliburton, L.E.; Nagashio, K.; Feigelson, R.S.; Schunemann, P.G. Electron paramagnetic resonance of Cr^{2+} and Cr^{4+} ions in $CdGeAs_2$ crystals. *J. Appl. Phys.* **2003**, *94*, 7567–7570. [CrossRef]
16. Yu, Y.; Zhao, B.; Zhu, S.; Gao, T.; Hou, H.; He, Z. Ab initio study of the linear and nonlinear optical properties of chalcopyrite $CdGeAs_2$. *J Solid State Chem.* **2012**, *185*, 264–270. [CrossRef]
17. Ma, C.G.; Krasnenko, V.; Brik, M.G. Effects of composition on the properties of mixed $CdSi_{1-x}Ge_xAs_2$ chalcopyrites as explored by the first-principles calculations. *Mater. Des.* **2017**, *126*, 250–258. [CrossRef]
18. Yu, M.; Xiao, X.; Xiong, Z.; Li, J.; Liu, X.; Huang, W.; Chen, B.; He, Z. Structural, electronic and optical properties of $CdGeAs_2$ with hybrid density functional (HSE06). *Mater. Today Commun.* **2022**, *31*, 103276. [CrossRef]
19. Bai, L.; Schunemann, P.G.; Pollak, T.M.; Giles, N.C. Luminescence study of donors and acceptors in $CdGeAs_2$. *Opt. Mater.* **2004**, *26*, 501–505. [CrossRef]
20. Ernzerhof, M.; Scuseria, G.E. Assessment of the Perdew–Burke–Ernzerhof exchange-correlation functional. *J. Chem. Phys.* **1999**, *110*, 5029–5036. [CrossRef]
21. Moussa, J.E.; Schultz, P.A.; Chelikowsky, J.R. Analysis of the Heyd-Scuseria-Ernzerhof density functional parameter space. *J. Chem. Phys.* **2012**, *136*, 204117. [CrossRef] [PubMed]
22. Jaffe, J.E.; Zunger, A. Theory of the band-gap anomaly in ABC_2 chalcopyrite semiconductors. *Phys. Rev. B* **1984**, *29*, 1882–1906. [CrossRef]
23. Marenkin, S.F.; Novotortsev, V.M.; Palkina, K.K.; Mikhailov, S.G.; Kalinnikov, V.T. Preparation and structure of $CdGeAs_2$ crystals. *Inorg. Mater.* **2004**, *40*, 135–137. [CrossRef]
24. Hafner, J. Ab-Initio Simulations of Materials Using VASP: Density-Functional Theory and Beyond. *J Comput Chem.* **2008**, *29*, 2044–2078. [CrossRef]
25. Tomas, B.; Jurgen, H.; Sebastien, L.; Janos, G.A. Improved Description of the Structure of Molecular and Layered Crystals: Ab Initio DFT Calculations with van der Waals Corrections. *J. Phys. Chem. A* **2010**, *114*, 11814–11824.
26. Abrahams, S.C.; Bernstein, J.L. Piezoelectric nonlinear optic $CuGaSe_2$ and $CdGeAs_2$: Crystal structure, chalcopyrite microhardness, and sublattice distortion. *J. Chem. Phys.* **1974**, *61*, 1140–1146. [CrossRef]
27. Isomura, S.; Takahashi, S.; Masumoto, K. Electrical and optical properties of $CdGeAs_2$. *J. Appl. Phys.* **1977**, *16*, 1723. [CrossRef]
28. Limpijumnong, S.; Lambrecht, W.R.L. Band structure of $CdGeAs_2$ near the fundamental gap. *Phys. Rev. B.* **2002**, *65*, 165204. [CrossRef]

29. El Moctar, C.O.; Kambas, K.; Marsillac, S.; Anagnostopoulos, A.; Bernede, J.C.; Benchouck, K. Optical properties of $CuAlX_2$ (X=Se, Te) thin films obtained by annealing of copper, aluminum and chalcogen layers sequentially deposited. *Thin Solid Film.* **2000**, *371*, 195–200. [CrossRef]
30. Polygalov, Y.I.; Poplavnoi, A.S. Energy band sturcture of $CdSnAs_2$ and $CdGeAs_2$. *Russ. Phys. J.* **1981**, *24*, 1139–1142.
31. Tauc, J. Optical properties and electronic structure of amorphous Ge and Si. *Mat. Res. Bull.* **1968**, *3*, 37–46. [CrossRef]
32. Pandey, R.; Ohmer, M.; Gale, J. A theoretical study of native acceptors in $CdGeAs_2$. *J. Phys. Condens. Matter* **1998**, *10*, 5525–5533. [CrossRef]
33. Kang, L.; Zhou, M.; Yao, J.; Lin, Z.; Wu, Y.; Chen, C. Metal Thiophosphates with Good Mid-Infrared Nonlinear Optical Performances: A First-Principles Prediction and Analysis. *J. Am. Chem. Soc.* **2015**, *137*, 13049–13059. [CrossRef] [PubMed]
34. Boyd, G.; Buehler, E.; Storz, F.; Wernick, J. Linear and nonlinear optical properties of ternary $A^{II}B^{IV}C_2{}^{V}$ chalcopyrite semiconductors. *IEEE J. Quantum Electron.* **1972**, *8*, 419–426. [CrossRef]